AD-A268 616

ATION PAGE

Form Approved
OMB No. 0704-0188

1. AGENCY USE ONLY (Leave blank)	2. REPORT DATE	3. REPORT TYPE AND DATES COVERED
	17 March 1993	Reprint

4. TITLE AND SUBTITLE
Recombinant Human Butyrylcholinesterase G390V, The Fluoride-2 Variant, Expressed in Chinese Hamster Ovary Cells, Is a Low Affinity Variant

5. FUNDING NUMBERS
Grant No.
DAMD17-91-Z-1003

61102A
3M161102BS11.AA.013
WUDA335680

6. AUTHOR(S)
Patrick Masson, Steve Adkins, Patrice Gouet
Oksana Lockridge

7. PERFORMING ORGANIZATION NAME(S) AND ADDRESS(ES)
University of Nebraska Medical Center
600 S. 42nd Street
Omaha, NE 68198-6805

8. PERFORMING ORGANIZATION REPORT NUMBER

9. SPONSORING / MONITORING AGENCY NAME(S) AND ADDRESS(ES)
U.S. Army Medical Research & Development Command
Fort Detrick
Frederick, Maryland 21702-5012

10. SPONSORING / MONITORING AGENCY REPORT NUMBER

11. SUPPLEMENTARY NOTES
Contract Title: Expression of Recombinant Butyrylcholinesterase in Mammalian Cells

12a. DISTRIBUTION / AVAILABILITY STATEMENT
Approved for public release; distribution unlimited

12b. DISTRIBUTION CODE

13. ABSTRACT *(Maximum 200 words)*

14. SUBJECT TERMS	15. NUMBER OF PAGES
RA V, Reprint, Genes, Nucleic Acids	16. PRICE CODE

17. SECURITY CLASSIFICATION OF REPORT	18. SECURITY CLASSIFICATION OF THIS PAGE	19. SECURITY CLASSIFICATION OF ABSTRACT	20. LIMITATION OF ABSTRACT
Unclassified	Unclassified	Unclassified	N/A

DISCLAIMER NOTICE

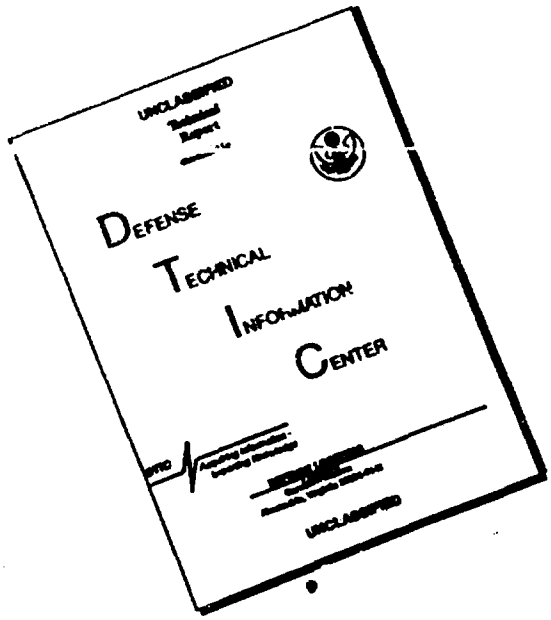

THIS DOCUMENT IS BEST QUALITY AVAILABLE. THE COPY FURNISHED TO DTIC CONTAINED A SIGNIFICANT NUMBER OF PAGES WHICH DO NOT REPRODUCE LEGIBLY.

THE JOURNAL OF BIOLOGICAL CHEMISTRY
© 1993 by The American Society for Biochemistry and Molecular Biology, Inc.

Vol. 268, No. 19, Issue of July 5, pp. 14329-14341, 1993
Printed in U.S.A.

Recombinant Human Butyrylcholinesterase G390V, the Fluoride-2 Variant, Expressed in Chinese Hamster Ovary Cells, Is a Low Affinity Variant*

(Received for publication, January 25, 1993, and in revised form, March 17, 1993)

Patrick Masson‡, Steve Adkins§, Patrice Gouet¶, and Oksana Lockridge‖**

From the ‡Centre de Recherches du Service de Santé des Armées, Unité de Biochimie, 24, Avenue des Maquis du Grésivaudan, B. P. 87 38702 La Tronche Cedex, France, the §Toxicology Department, University of Michigan Medical School, Ann Arbor, Michigan, 48109, the ¶Institut de Biologie Structurale, Laboratoire de Cristallographie Macromoléculaire, Grenoble 38027, France, and the ‖Eppley Institute, University of Nebraska Medical Center, Omaha, Nebraska 68198-6805

Kinetics of recombinant fluoride-2 variant of human tyrylcholinesterase (Gly^{390} Val) secreted by Chinese mster ovary cells were compared to recombinant ual and to usual butyrylcholinesterase purified from man plasma. The usual and fluoride-2 variant were distinguishable with regard to hydrolysis of benylcholine (K_m = 5 μM), neutral esters, and at high ncentrations of acetylthiocholine, propionylthiocholine, and butyrylthiocholine. However, at low subrate concentrations K_m values for acetylthiocholine id succinyldithiocholine were 2–6-fold higher for the uoride-2 variant. pH rate profiles revealed small differences in pK_a that could be attributed to changes in ie active site histidine environment. On the other and, Arrhenius plot analysis of *o*-nitrophenylbutyrate ydrolysis at pH 7.5 showed no difference in activation nergy between fluoride-2 and usual butyrylcholinesterases. Both exhibited an anomalous temperature dependence with a wavelike change in activation energy around 18 °C. Affinity of the fluoride-2 variant for sodium fluoride, tacrine, dibucaine, amodiaquin, and succinyldicholine was lower than for usual enzyme. Apparent K_i for succinyldicholine was 125 μM for the fluoride-2 variant and 20 μM for the usual enzyme. Organophosphate inhibition showed equivalent reactivity, indicating that the point mutation altered only the binding properties of the variant. Thus, K_m and K_i changes explain the succinyldicholine sensitivity of people carrying the fluoride-2 variant.

The synthesis of human butyrylcholine esterase (EC 3.1.1.8) is directed by a single gene, named BCHE[1] (1–3). Butyrylcholinesterase (BuChE) is present in almost all tissues, with the exception of lymphocytes and placenta. It is secreted into plasma by liver cells. Unlike its sister enzyme, AChE, no physiological function has yet been assigned to BuChE, but the plasma enzyme is of pharmacological importance because it hydrolyzes ester-containing drugs (4). The BCHE gene is known to include at least 10 genetic variants (5). Some of the rare alleles encode variants that are unable to hydrolyze the muscle relaxant succinyldicholine in a short time (4, 6). People carrying these variants experience an exaggerated response to succinyldicholine. Two of these variants are phenotyped by resistance to inhibition by 50 μM NaF (7). The fluoride-1 variant results from a point mutation at nucleotide 728 that changes threonine 243 to methionine. The fluoride-2 variant has a point mutation at nucleotide 1169 which changes glycine 390 to valine (8). Fluoride-2 is more frequent than fluoride-1 (8). The incidence of the homozygous fluoride phenotype in Caucasians is approximately 1 out of 150,000 (6). The scarcity of the homozygous fluoride variant has made it difficult to study this variant, and almost nothing is known about the effects of the mutation on the properties of the enzyme.

To understand the effect of the Gly^{390} to Val point mutation on the activity of BuChE, we expressed the fluoride-2 BCHE gene and the wild-type (usual) BCHE gene in CHO cells. The present work compares the kinetic properties of recombinant fluoride-2 BuChE with recombinant usual BuChE and with purified usual plasma BuChE.

MATERIALS AND METHODS

Purified Human Plasma BuChE—Human plasma BuChE was purified to 90% purity in two steps (4). The enzyme was assayed according to Kalow and Lindsay (9) in 0.067 M Na/K phosphate buffer, pH 7.4, at 25 °C with 50 μM benzoylcholine chloride (Sigma) as the substrate. Benzoylcholine hydrolysis was followed by monitoring decrease in absorbance at 240 nm ($\Delta\epsilon$ = 6700 M^{-1} cm^{-1}). The specific activity of the preparation was 180 units/mg protein (1 unit = 1 μmol of benzoylcholine hydrolyzed/min). The enzyme had the "usual" phenotype.

CHO Cell Line Secreting Fluoride-2 Variant of Human Butyrylcholinesterase—Human cDNA encoding a 28-amino-acid signal peptide and 574 amino acids of the mature BuChE enzyme was cloned into the pD5 expression vector where expression is controlled by the adenovirus major late promoter (10). This cDNA had a substitution which changed Gly^{390} (GGT) to Val (GTT), the mutation responsible for the fluoride-2 variant (8). The mutation was present in cDNA isolated from a human brain library (11) and therefore shows that the donor was a carrier of the fluoride-2 mutation BCHE*390V. A stable cell line expressing human BuChE was created by cotransfecting pD5-BCHE and pD5-dihydrofolate reductase into CHO cells doubly deficient for dihydrofolate reductase. The deficient CHO cells, DG44, were kindly provided by L. A. Chasin (12). The BCHE and

* This work was supported by grants from the United States Army Medical Research and Development Command DAMD17-91-Z-1003 (to O. L), La Direction des Recherches, Etudes et Techniques DRET 91/1044 J (to P. M), American Cancer Society Grants SIG-16A and IRG-165E, and National Cancer Institute Grant P30 CA 36727 (to The Eppley Institute). The costs of publication of this article were defrayed in part by the payment of page charges. This article must therefore be hereby marked "*advertisement*" in accordance with 18 U.S.C. Section 1734 solely to indicate this fact.

** To whom correspondence should be addressed: Eppley Institute, University of Nebraska Medical Center, 600 S. 42nd St., Omaha, NE 68198-6805. Tel.: 402-559-6032; Fax: 402-559-4651.

[1] The abbreviations used are: BCHE, butyrylcholinesterase gene; AChE, acetylcholinesterase enzyme; BuChE, butyrylcholinesterase enzyme; CHO, Chinese hamster ovary cells; FF, homozygous fluoride-2 butyrylcholinesterase enzyme; iso-OMPA, tetraisopropylpyrophosphoramide; UU, homozygous usual butyrylcholinesterase enzyme; 3-D, three-dimensional.

dihydrofolate reductase genes became amplified approximately 100-fold in response to increasing doses of methotrexate. The stable cell line was maintained under selective pressure by growing cells in minimum essential medium-α, with L-glutamine, without ribonucleosides and deoxyribonucleosides (GIBCO Catalog No. 320-2561AJ) containing 10% dialyzed fetal calf serum. BuChE was collected into serum-free medium, CHO-S-FM (GIBCO 320-2050AJ) because it has only 0.4% of the bovine AChE present in fetal calf serum. The benzoylcholine activity of secreted rBuChE fluoride-2 variant was 0.04 units/ml.

CHO Cell Line Secreting Usual Human Butyrylcholinesterase—The cDNA sequence of human BCHE was modified by site-directed mutagenesis to give the optimal start site context as identified by Kozak (13). The optimal start site sequence is GCCACCATGG where ATG is the translation initiation codon. Two *Bgl*II restriction sites were introduced at the 5′ and 3′ ends of the coding sequence to have the shortest possible cDNA free of extraneous sequences that might interfere with translation efficiency. The *Bam*HI site at Gly^{225} was removed. After site-directed mutagenesis, the BCHE gene was completely resequenced to ensure the absence of unwanted mutations. The 1.8-kilobase BCHE gene was cloned into plasmid pRcCMV (Invitrogen) where expression is controlled by the cytomegalovirus promoter. Ten μg pRcCMV-BCHE was transfected into CHO DG44 cells by calcium phosphate coprecipitation. Cells resistant to 0.8 mg/ml geneticin (GIBCO 860-1811 II) were selected over a 3-week period. Clonal cell lines were created by diluting resistant cells into 96-well plates at less than 1 cell/well. Cells secreting the highest level of BuChE activity, as measured with benzoylcholine, were expanded into T75 flasks. Cells were grown to 90% confluence in a T75 flask in the presence of complete medium containing 10% fetal calf serum. Culture medium was replaced with CHO-S-FM containing 0.8 mg/ml geneticin for the purpose of collecting BuChE into serum-free medium. Cells were continuously cultured in CHO-S-FM for 3 months. The secreted rBuChE reached an activity of 0.5 units/ml which is nearly the activity in human plasma.

Activity Versus pH—The pH dependence of enzyme activity (k_{obs}) was investigated at 25 and 41 °C in 0.067 M potassium phosphate buffer in the pH range 5.5 to 8.98. Various ratios of 0.067 M KH_2PO_4 and 0.067 M K_2HPO_4 were mixed to get buffers that varied in pH but had the same concentration. Activity was measured with 50 μM benzoylcholine, a concentration 10 times the K_m value determined at pH 7.4, 25 °C.

In parallel, the pH dependence of enzyme inhibition by 50 μM NaF was measured in the same pH range in the presence of 50 μM benzoylcholine. The substrate and inhibitor concentrations were chosen on the basis of differential inhibition of usual and "fluoride-resistant" BuChE phenotypes: with these concentrations, the difference between the percentage inhibition by sodium fluoride of usual and fluoride BuChE is maximum (7, 14).

The pH rate profile for k_{obs} of BuChE-catalyzed hydrolysis of benzoylcholine was interpreted according to the simplest model which assumes that H^+ acts as an uncompetitive inhibitor, *i.e.* the protonated form of the enzyme is completely unreactive.

$$k_{obs} = \frac{k_{obs\,max} \cdot K_a}{K_a + [H^+]} \qquad \text{(Eq. 1)}$$

In Equation 1, $k_{obs\,max}$ is the maximum value of k_{obs} at high pH, and K_a is the ionization constant of an amino acid side chain whose deprotonated form takes part in catalysis.

Apparent pK_a values were computer-calculated by nonlinear regression fitting of the experimental data to Equation 1. We used the GraFit (version 1.0) pH GFE curve fitting program (Erithacus Software Ltd, United Kingdom, 1989).

Kinetics of Substrate Hydrolysis—Kinetic analyses were performed in 0.067 M phosphate buffer, pH 7.0, 7.5, or 8.0 at 25 °C. Hydrolysis of acetylthiocholine iodide, propionylthiocholine iodide, butyrylthiocholine iodide, and succinyldithiocholine iodide (Molecular Probes Inc., Eugene, OR) was followed at 420 nm using the method of Ellman *et al.* (15). Substrate concentrations ranged from 0.006 to 3 mM. Hydrolysis of benzoylcholine was followed by recording the decrease in absorbance at 240 nm. Hydrolysis of *o*-nitrophenylacetate and *o*-nitrophenylbutyrate was followed by monitoring the rate of appearance of *o*-nitrophenol at 410 nm ($\epsilon = 3190\ M^{-1}\ cm^{-1}$). Hydrolysis of α-naphthylacetate and α-naphthylbutyrate was measured by the method of Zapf and Coghlan (16) by recording the increase in absorbance at 321 nm (α-naphthol, $\epsilon = 2220\ M^{-1}\ cm^{-1}$). Stock solutions of *o*-nitrophenylacetate and *o*-nitrophenylbutyrate were prepared in methanol; the methanol concentration in each reaction cuvette was maintained at 5.3%. Stock solutions of α-naphthylacetate and α-naphthylbutyrate were prepared in ethanol; the ethanol concentration in each reaction cuvette was maintained at 3.33%.

K_m and V_{max} Determinations—Kinetic data were plotted using the Lineweaver-Burk double-reciprocal plot. The enzymes had either Michaelian or nonMichaelian behavior depending on the nature of the substrate. For Michaelian behavior, K_m and V_{max} were determined by nonlinear regression of the Michaelis-Menten equation using the Enzfitter kinetic calculation program (Biosoft, Cambridge, UK). For nonMichaelian behavior (curvatures in the Lineweaver-Burk plots), the apparent K_m and V_{max} were estimated graphically from the linear sections of the curves.

Temperature Dependence of o-Nitrophenylbutyrate Hydrolysis Rate—The temperature dependence of BuChE-catalyzed hydrolysis of *o*-nitrophenyl butyrate (0.8 mM in 0.067 M phosphate buffer, pH 7.5, containing 5.3% methanol) was determined at various temperatures from 10 to 50 °C. The reaction rate (k) was measured at intervals of 1-2 °C. We operated at nearly saturating substrate concentration, at 0.8 mM which is four times higher than K_m. Observed reaction rates were corrected for spontaneous substrate hydrolysis. Arrhenius plots were obtained by plotting ln k against 1/T, where T is the absolute temperature. The experimental activation energies E were calculated from the slopes of the linear portions of the plots by linear regression analysis.

Reversible Inhibition—Inhibition by NaF was performed in 0.067 M phosphate, pH 7.0 and 8.0, at 25 °C with benzoylcholine as the substrate. Inhibition by succinyldicholine chloride (Sigma), tacrine (tetrahydroaminoacridine), dibucaine, and amodiaquin was carried out in 0.067 M phosphate, pH 7.5, at 25 °C with *o*-nitrophenylacetate as the substrate (all compounds were from Sigma). Inhibition by amodiaquin was also carried out at pH 7.0 with butyrylthiocholine iodide as the substrate. Types of inhibition and apparent inhibition constants were determined from Lineweaver-Burk plots and Dixon plots (17) by plotting the reciprocal of velocity [v^{-1}] against inhibitor concentration [I]. Inhibition constants for nonlinear inhibition were calculated from replots of the reciprocals of slopes and intercepts of the Lineweaver-Burk plots against the reciprocal of inhibitor concentration (17).

Progressive Inhibition—Progressive inhibition by eserine (0.5, 1, 10 μM) was conducted in 0.1 M phosphate, pH 7.0, at 25 °C. Residual activity was measured in 0.067 M phosphate, pH 7.5, with *o*-nitrophenylacetate (0.8 mM) as substrate. Progressive inhibition by tetraisopropylpyrophosphoramide (iso-OMPA) was either performed as above or after 1 h of incubation of BuChE in 0.1 M phosphate, pH 7.0, containing 5 mM EDTA as an inhibitor of metal proteases and organophosphate hydrolase. The iso-OMPA concentrations ranged from 10 to 200 μM. Residual activity was measured by Ellman's method (15) with butyrylthiocholine iodide (1 mM) as substrate.

Inhibition by eserine or iso-OMPA (I) results in carbamylation or phosphorylation of the enzyme active site serine (E) according to Scheme I:

$$E + I \underset{k_{-1}}{\overset{k_1}{\rightleftarrows}} E \cdot I \xrightarrow{k_2} EI' \xrightarrow[H_2O]{k_3} E$$

SCHEME I

where $K_i = k_{-1}/k_1$ is the dissociation constant of the enzyme-inhibitor complex and k_2 the rate constant of carbamylation or phosphorylation. The rate constant of hydrolysis, k_3, is very slow. Assuming that the enzyme is irreversibly inhibited under the conditions of the experiments, the activity (e_t/e_o) decreases with time (t) as follows,

$$\frac{e_t}{e_o} = e^{-k_i t} \qquad \text{(Eq. 2)}$$

where k_i is the apparent inhibition rate constant.

Since $[I] >> e_o$ and assuming that the rapid equilibrium condition, $k_2 << k_{-1}$, holds (18), the apparent rate of inactivation can be written as:

$$k_i = \frac{k_2}{1 + \frac{K_i}{[I]}} \qquad \text{(Eq. 3)}$$

The value of the inactivation rate constant (k_i) was determined for each inhibitor concentration by weighted exponential regression of

Equation 2. Then k_2 and K_i were determined by weighted nonlinear regression fitting of Equation 3 using the Enzfitter program.

Molecular Modeling—Three-dimensional models of wild-type and the fluoride-2 variant of human BuChE were built from the 3-D coordinates of *Torpedo californica* AChE (19) by molecular replacement and energy minimization using the molecular modeling package TURBO-FRODO 4.0 (20) and the refinement program X-PLOR 3.0 (21). Analysis of 3-D models was carried out on a Silicon Graphics 310GTX workstation.

3-D structures of succinyldicholine (22) and dibucaine (23) were obtained from the Cambridge Structural Database (24, 25). The 3-D structure of *o*-nitrophenylacetate was built from the 3-D structure of *p*-nitrophenylacetate (26) which is in the Cambridge Structural Database. Topology and energy parameters of these compounds were computed from Cambridge Structural Database data and by using the X-PLOR "prolsq.pro" file. This file allowed optimization of substrate and ligand geometry in the BuChE active site. Structures of substrate and ligand BuChE complexes were refined using the X-PLOR program after inspection of substrate and ligand noncovalent bonds with BuChE and generation of the BuChE accessibility surface. The solvent-accessible molecular surface was represented as a smooth continuous lattice of points using Connolly's program MS (27). All these refinements were carried out by molecular dynamics at 300 K and conjugate gradient method with a convergence criterion of 1.5 kcal/mol/Å.

RESULTS

Kinetics of Substrate Hydrolysis—Hydrolysis of neutral esters followed Michaelis-Menten kinetics, giving a linear relationship between the reciprocal of activity and the reciprocal of ester concentration for both fluoride-2 and usual BuChE. Table I shows that fluoride-2 BuChE (rFF) had a slightly lower affinity for neutral substrates, with K_m at most 1.5 times higher for fluoride-2 BuChE than for usual BuChE.

Hydrolysis of charged esters was more complex, with benzoylcholine giving the simplest kinetics. The kinetics of hydrolysis of benzoylcholine were Michaelian, but as previously shown, usual BuChE displayed substrate inhibition at benzoylcholine concentrations greater than 50 μM when assayed at pH 7.0 (34, 35). The substrate inhibition constant K_{ss} was determined according to the Haldane equation:

$$v = \frac{V_{max}}{1 + \frac{K_m}{[S]} + \frac{[S]}{K_{ss}}} \qquad \text{(Eq. 4)}$$

K_{ss} was found to be 500 μM at pH 7.0 and at pH 8.0 for both recombinant usual and purified usual plasma BuChE. No substrate inhibition was observed for fluoride-2 BuChE except at pH 8.0 in the presence of 0.05–2 mM NaF. Usual and fluoride-2 BuChE had nearly the same affinity for benzoylcholine, both having K_m values of approximately 5 μM (Table II).

Hydrolysis of thiocholine esters was the most complex. Usual and fluoride-2 BuChE both deviated from the simple Michaelis-Menten model when the substrates were thiocholine esters. For example, Fig. 1 shows biphasic kinetics for the hydrolysis of butyrylthiocholine. It has been known for many years (40) that these biphasic kinetics reflect activation at high substrate concentration. A least two mechanistic models can account for this activation: the first one assumes binding of an additional substrate molecule to the acyl-enzyme intermediate (41); the second hypothesizes the existence of a peripheral regulatory binding site for charged ligands or substrates (42). Lineweaver-Burk plots allowed us to estimate apparent K_m values for high and low substrate concentrations (Table II). At high substrate concentration the K_{m2} values for acetylthiocholine, propionylthiocholine, butyrylthiocholine, and succinyldithiocholine were practically the same for both usual and fluoride-2 BuChE. On the other hand, at low substrate concentration, the ratio of K_{m1} values showed that affinity of fluoride-2 BuChE for acetylthiocholine and succinyldithiocholine esters was two to three times lower than that of usual BuChE. A more refined description of the kinetics of acetylthiocholine, propionylthiocholine, and butyrylthiocholine hydrolysis was possible using the general mathematical expression proposed for the two above-mentioned models (42):

$$V = \frac{V_m[S] + V_m' \frac{[S]^2}{K_2}}{K_1 + [S] + \frac{[S]^2}{K_2}} \qquad \text{(Eq. 5)}$$

where $V_m' = aV_m$ with $a > 1$. Equation 5 was used to calculate V_m, V_m', K_1, and K_2 in Table III. A comparison of K_{m1} and K_{m2} in Table II with K_1 and K_2 in Table III shows that values for K_{m1} are very close to values for K_1, and values for K_{m2} are very close to values for K_2. Thus, the graphic analysis to calculate K_m1 and K_{m2} in Table II yielded similar results as the computer analysis to calculate K_1 and K_2 in Table III. In Table III the K_1 and K_2 ratios decrease in parallel as the size of the acid moiety of the substrates increases. The conclusion from the data in Tables II and III is that there are no major kinetic differences between usual BuChE and fluoride-2 BuChE. The point mutation in the fluoride-2 variant does not change the mechanism of hydrolysis of thiocholine esters.

The K_m values for succinyldithiocholine for usual and fluoride-2 BuChE are of special interest because of the clinical problems associated with use of succinyldicholine in people who have the fluoride-2 variant. Table II shows that the K_m1 values for fluoride-2 BuChE are 3.5- and 1.6-fold higher than for usual BuChE at pH 7.0 and 8.0, respectively. It is reason-

TABLE I

K_m values for neutral substrates of purified BuChE from human plasma (UU), recombinant fluoride-2 BuChE (rFF), and recombinant usual BuChE (rUU)

Substrate	K_m					Comment
	pH[a]	UU	rFF	ratio	rUU	
			mM			
o-Nitrophenylacetate	7.5	0.48 ± 0.16	0.45 ± 0.19	1	0.38 ± 0.01	In the presence of 5.3% methanol
o-Nitrophenylbutyrate	7.5	0.125 ± 0.02[b]	0.185 ± 0.03	1.5		
α-Naphthylacetate	7.0	0.34[c]	0.41	1.2		In the presence of 3.33% ethanol
α-Naphthylbutyrate	7.0	0.044	0.068	1.5		

[a] 0.067 M phosphate, 25 °C.

[b] Literature values for K_m for *o*-nitrophenylbutyrate: 0.14 mM in 0.067 M phosphate, pH 7.4 (28, 29); 0.19 mM in 50 mM phosphate, pH 7.6 (30); 0.14 mM in 50 mM phosphate, pH 7.6, 25 °C (31); 0.33 mM in 0.1 M Tris-Cl, pH 7.4, 25 °C (33).

[c] Literature values for K_m for α-naphthylacetate: 0.76 mM in 50 mM Tris-Cl, pH 7.4, 37 °C (32); 1.0 mM in 0.1 M Tris-Cl, pH 7.4, 25 °C (33).

TABLE II

Kinetic parameters for positively charged substrates of purified BuChE from human plasma (UU), recombinant usual BuChE (rUU), and recombinant fluoride-2 BuChE (rFF)

Substrate	pH[a]	Michaelian behavior K_m			Non-Michaelian behavior					
					K_{m1}, low [S]			K_{m2}, high [S]		
		UU	rUU	rFF	UU	rUU	rFF	UU	rUU	rFF
					mM					
Benzoylcholine	7	0.0044[b] ±0.0007	0.0069	0.0075 ±0.0044						
Benzoylcholine	8	0.0041[b] ±0.0006	0.0034	0.0052 ±0.0012						
Acetylthiocholine	7				0.049[c] ±0.007	0.019	0.091 ±0.047	0.49 ±0.24	0.29	0.49 ±0.23
Propionylthiocholine	7				0.024 ±0.007	0.022	0.029	0.42 ±0.03	0.22	0.31 ±0.12
Butyrylthiocholine	7				0.023[d] ±0.014	0.022	0.027 ±0.004	0.26[d] ±0.001	0.19	0.16 ±0.01
Succinyldithiocholine	7				0.0020[e]	0.0020	0.0069	3.83 ±0.23	4.65	4.39 ±0.55
Succinyldithiocholine	8				0.0019[e]	0.0020	0.0033	2.08 ±0.58	1.53	2.13 ±0.51

[a] 0.067 M phosphate, 25 °C.

[b] Literature values for K_m for benzoylcholine: 0.005 mM in 0.067 M phosphate, pH 7.4, 25 °C (34); 0.004 mM in 0.067 M phosphate, pH 7.4, 25 °C (4, 35); 0.0034 mM in 50 mM phosphate, pH 7.2, 30 °C (36).

[c] Literature values for K_m for acetylthiocholine: 0.043 and 0.29 mM in 50 mM Tris-Cl, pH 7.4, 30 °C (37).

[d] Literature values for K_m for butyrylthiocholine: 0.055 and 2.0 mM in 0.1 M MOPS/KOH, pH 7.0, 30 °C (38); 0.018 and 0.24 mM in 50 mM Tris-Cl, pH 7.4, 30 °C (37); 0.024 mM in 50 mM phosphate, pH 7.2, 30 °C (36).

[e] Literature values for K_m for succinyldithiocholine: 0.0034 mM in 50 mM Tris-Cl, pH 7.4, 30 °C (37); 0.032 mM in 50 mM Tris-Cl, pH 7.4, 30 °C (37, 39).

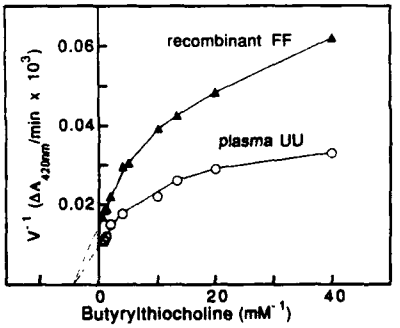

FIG. 1. **Lineweaver-Burk plot for BuChE-catalyzed hydrolysis of butyrylthiocholine.** Activity was measured in 0.1 M phosphate buffer, pH 7.0, at 25 °C. Velocity is expressed as the reciprocal (V^{-1}) of the change in absorbance at 420 nm/min recombinant fluoride-2 BuChE, FF (Δ); purified usual plasma BuChE, UU (O). At high substrate concentration, K_m = 0.25 mM for both recombinant FF and plasma UU.

able to propose that a 2–3-fold difference in K_m explains the succinyldicholine sensitivity of people carrying the fluoride variant.

pH Dependence of the Hydrolysis of Benzoylcholine—The effect of pH upon enzyme activity near V_{max} was investigated at pH values ranging from 5.5 to 8.98 and at two temperatures, 25 and 41 °C (Fig. 2). Experimental data were fitted to Equation 1 for determination of apparent pK_a. The observed pK_a values of 7.26 for usual BuChE and 7.03 for recombinant fluoride-2 BuChE at 25 °C are in agreement with the known pK_a of the histidine ring.

The apparent enthalpy of ionization, ΔH, was calculated from pK_a values at 25 and 41 °C using the Van't Hoff equation, by assuming a linear temperature dependence of pK_a. The ΔH value for usual BuChE was 27.9 kJ mol^{-1}, a value consistent with ΔH for ionization of histidine, which is known to have ΔH values of 28–31 kJ mol^{-1}. The ΔH value for fluoride-2 BuChE was significantly lower, 15.6 kJ mol^{-1}, and may reflect a change in the immediate environment of histidine to a more hydrophobic environment, thus tending to destabilize the imidazole ring. The histidine measured by these pK_a and ΔH values was assumed to be the histidine in the catalytic triad, His^{438}, by analogy with *Torpedo* AChE (19, 43, 44).

Temperature Dependence of the Hydrolysis of o-Nitrophenylbutyrate—The temperature-dependence of BuChE-catalyzed hydrolysis of *o*-nitrophenyl butyrate at v = approximate V_{max}, measured at *o*-nitrophenylbutyrate concentration about 5-fold higher than K_m, is identical for the usual enzyme (plasma or recombinant) and fluoride-2 BuChE. As shown in Fig. 3, the Arrhenius plot is nonlinear and exhibits a wavelike discontinuity at 18 °C. In an earlier experiment with usual BuChE, a clear break in the Arrhenius plot was observed at 21 °C in the presence of 0.5% methanol (29). This was ascribed to a temperature-induced conformational change. In Fig. 3 the wavelike break may be interpreted as the coexistence of two active conformations in equilibrium in a narrow temperature interval around 18 °C. A break at 18 °C rather than at 21 °C is due to the higher methanol concentration of 5.3%. The activation energy (*Ea*) required for substrate hydrolysis is different on both sides of the discontinuity but there is no significant difference between the three enzymes. In the temperature range 10–17 °C, *Ea* is 71.8 ± 9.4 kJ mol^{-1}; between 18 and 38 °C it is 44.8 ± 4.5 kJ mol^{-1}. Beyond 38 °C the activity of the recombinant usual enzyme drops rapidly. The heat sensitivity of this enzyme is due to proteolytic nicks. The fact that the three enzymes exhibit the same temperature dependence indicates that their posttranslational modifications (glycosylation and proteolytic nicks) do not affect the catalytic step. Moreover, it appears that the G390V mutation has no effect on the activation step that precedes enzyme acylation by *o*-nitrophenylbutyrate.

Inhibition by Sodium Fluoride—The effect of sodium fluoride (50 μM) upon the pH dependence of benzoylcholine hydrolysis was examined. NaF shifted the pH activity curve in opposite directions for UU and rFF (Fig. 2, *panels 1* and

TABLE III

Kinetic parameters of purified usual (UU) plasma BuChE and recombinant fluoride-2 BuChE (rFF) calculated by nonlinear regression using equation 5

Substrate	pH[a]	UU				rFF				K_1 ratio	K_2 ratio
		V_m[b]	V'_m	K_1	K_2	V_m	V'_m	K_1	K_2		
		mM				mM					
Acetylthiocholine	7.0	19.2	51.9	0.033	0.62	11.3	26.8	0.072	1.21	2.2	1.9
Propionylthiocholine	7.0	34.8	77.5	0.024	0.41	8.8	67.3	0.027	0.63	1.1	1.5
Butyrylthiocholine	7.0	42.9	213.7	0.014	0.21	13.5	65.6	0.011	0.23	0.8	1.1

[a] 0.067 M phosphate, 25 °C.
[b] Velocity unit is $\Delta A_{420nm}/min \times 10^3$.

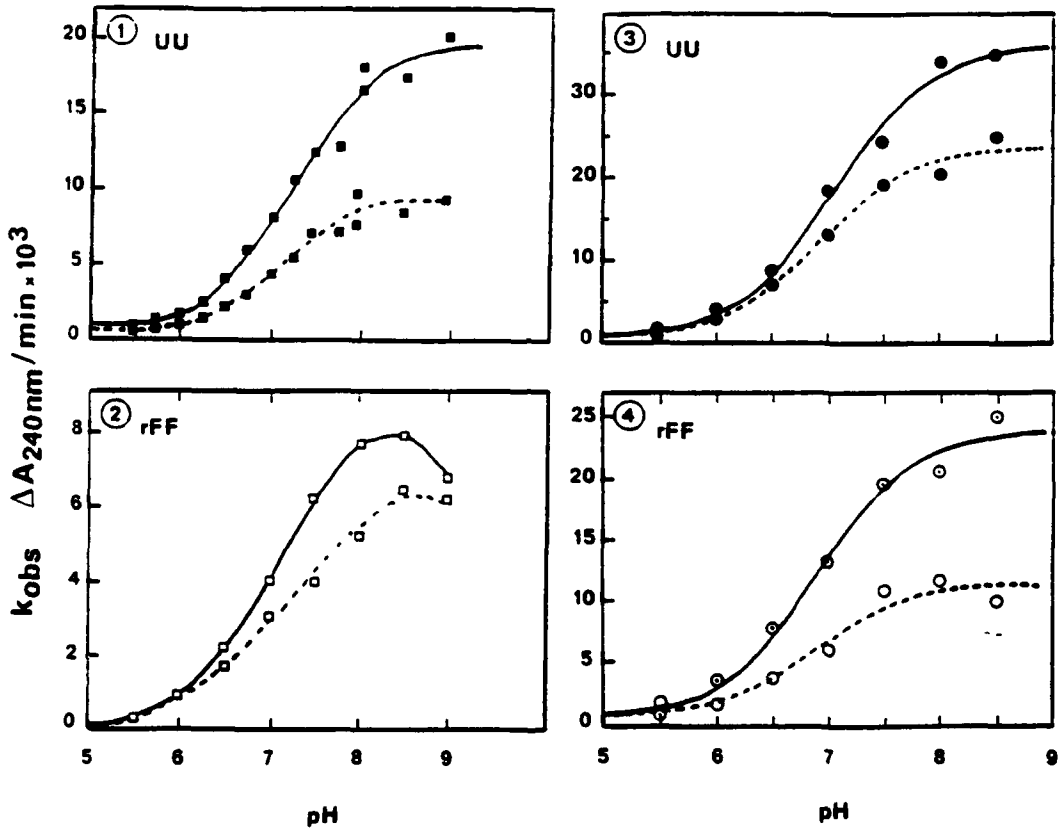

FIG. 2. **pH rate profiles for k_{obs} of BuChE-catalyzed hydrolysis of benzoylcholine at 25 and 41 °C.** *Panel 1*, purified usual plasma BuChE, UU, at 25 °C (■); *panel 2*, recombinant fluoride-2 BuChE, rFF, at 25 °C (□); *panel 3*, purified usual plasma BuChE, UU, at 41 °C (●); *panel 4*, recombinant fluoride-2 BuChE, rFF, at 41 °C (○). *Solid lines* are in the absence of inhibitor; *dashed lines* are in the presence of 50 μM NaF. k_{obs} was measured with 50 μM benzoylcholine in 0.067 M potassium phosphate buffer, pH 5.5–8.98, and is expressed as change in absorbance at 240 nm/min. Apparent pK_a values are: 7.26 ± 0.06 for UU at 25 °C, 7.05 ± 0.09 for UU at 41 °C, 7.03 ± 0.03 for rFF at 25 °C, 6.89 ± 0.11 for rFF at 41 °C. Apparent enthalpy of ionization values are: ΔH = 27.9 kJ mol^{-1} for usual BuChE, ΔH = 15.6 kJ mol^{-1} for recombinant fluoride-2 BuChE.

2). At 25 °C the apparent pK_a for UU shifted slightly to a lower pH (pK_a = 7.12 ± 0.10), whereas the apparent pK_a for rFF shifted to a higher pH (pK_a = 7.24 ± 0.06). At 41 °C (Fig. 2, *panels 3* and *4*), the apparent pK_a for UU shifted slightly to a lower pH (pK_a = 6.89 ± 0.11), whereas the apparent pK_a for rFF did not shift. Using acetylcholine, rather than benzoylcholine, and 5 mM NaF rather than 0.05 mM NaF, Heilbronn (45) as well as Brestkin and Fruentova (46) got results for usual BuChE that were the opposite of our results for UU in Fig. 2, *panel 1*. Heilbronn (45) found that in the presence of 5 mM NaF the pH activity curve was displaced toward a higher pH. This indicates a substrate-dependent kinetic behavior of BuChE.

As shown in Fig. 4, pH inhibition profiles differed widely for usual and fluoride-2 BuChE. At 25 °C usual BuChE was maximally inhibited by sodium fluoride at pH 8.0, whereas fluoride-2 BuChE was maximally inhibited at pH 7.5, a difference of 0.5 pH units. At 41 °C usual BuChE was maximally inhibited at pH 8.0, whereas fluoride-2 BuChE was maximally inhibited at pH 7.0, a difference of 1.0 pH units. For both usual and fluoride-2 BuChE percent inhibition by NaF was far greater at 25 than at 41 °C, confirming that inhibition by NaF is temperature sensitive (6, 7). At 25 °C and pH 7.4, the inhibition percentage (fluoride number) of the fluoride-2 recombinant enzyme was identical to the value (36%) given by the fluoride-resistant homozygote plasma enzyme (6). The inhibition percentage (fluoride number) of usual BuChE in Fig. 3 is 67%, a value similar to the average value of 60 for usual plasma BuChE (6).

Dixon plots for the inhibition of benzoylcholine hydrolysis

at pH 7.0 suggested that at low benzoylcholine concentration inhibition of fluoride-2 BuChE by sodium fluoride is uncompetitive with apparent $K_i \approx 0.3$ mM (Fig. 5, *panel 1*). However, at 25 μM benzoylcholine there was a deviation from simple uncompetitive inhibition in a fashion suggestive of a negative cooperative interaction similar to that seen by Page *et al.* (35) for usual BuChE. Page *et al.* (35) found that the binding of benzoylcholine is enhanced in the presence of fluoride ion with a cooperativity factor of 30. The inhibition mechanism of usual BuChE also appeared to be uncompetitive (apparent $K_i \approx 0.09$ mM) at low substrate concentration ([S] ≤ 10 μM), but the mechanism again changed at 25 μM benzoylcholine (Fig. 5, *panel 2*) in a manner indicative of cooperativity in the binding of fluoride ion and benzoylcholine, as expected for usual BuChE (35). Inspection of the 25 μM traces in *panels 1* and *2* of Fig. 5 showed that the rates up to 75 μM NaF are slower than would be expected for a simple uncompetitive mechanism. At NaF concentrations higher than 75 μM the traces differ, with the rFF enzyme showing a more shallow slope than the UU enzyme. This behavior is consistent with the switch point in the cooperative mechanism occurring at a higher fluoride concentration for the rFF enzyme. A weaker interaction between rFF and fluoride ion is also seen in the uncompetitive K_i values of 0.3 mM for rFF and 0.09 mM for UU. Fig. 5 (*panels 3* and *4*) shows that at pH 8.0, both usual and fluoride-2 BuChE exhibited substrate inhibition in the presence of NaF. At pH 8.0 inhibition was partially uncompetitive at low substrate concentration, but there was a synergistic effect between benzoylcholine and fluoride ion at high substrate concentration that amplified the inhibition. Due to the strong cooperativity in mutual binding of fluoride ion and benzoylcholine, Dixon plots were abnormal and could not lead to K_i estimation; nevertheless, they suggested that usual and fluoride-2 BuChE displayed a similar degree of cooperativity. Although inhibition by sodium fluoride has been known for many years (45), its mechanism has not yet been resolved and remains disconcerting.

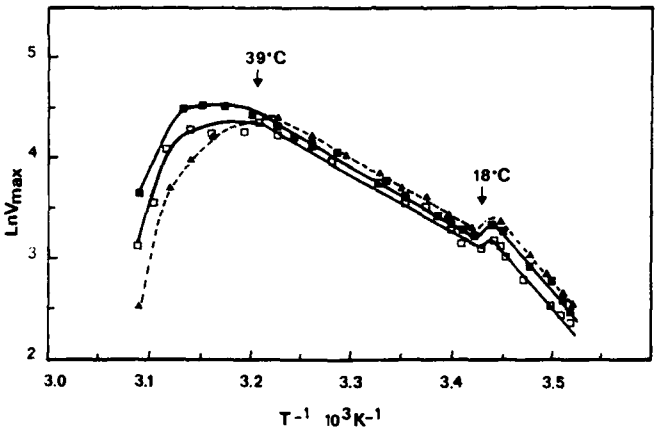

FIG. 3. **Arrhenius plots for BuChE-catalyzed hydrolysis of *o*-nitrophenylbutyrate.** Hydrolysis of 0.8 mM *o*-nitrophenylbutyrate in 0.067 M phosphate, pH 7.5, containing 5.3% methanol was measured at 1 to 2 degree temperature intervals. ■, purified usual plasma BuChE; ▲, recombinant usual BuChE; □, recombinant fluoride-2 BuChE. In the temperature range 10–17 °C, activation energy is 71.8 ± 9.4 kJ mol^{-1}; between 18 and 38 °C it is 44.8 ± 4.5 kJ mol^{-1}.

Reversible Inhibition by Positively Charged Ligands—Inhibition of *o*-nitrophenylacetate hydrolysis by dibucaine, tacrine, succinyldicholine, and amodiaquin was nonlinear for both usual and fluoride-2 BuChE, *i.e.* Dixon plots of v^{-1} *versus* [I] were downwardly curved, as shown for dibucaine in Fig. 6. This means that high inhibitor concentrations did not drive the reaction rate to zero. Apparent inhibition constants at low inhibitor concentration were estimated from Dixon plots and are given in Table IV. Fluoride-2 BuChE was less inhibited by these compounds than usual BuChE by a factor of 2.7–6.2 as shown by K_i ratios. Due to the strong deviation from linearity of these plots at high [I], neither the type of inhibition nor actual K_i could be simply determined. Partial nonlinear inhibition indicates that both *ES* and ternary complexes *ESI* yield products. Nonlinear reversible inhibition may be depicted by the following minimum reaction scheme II.

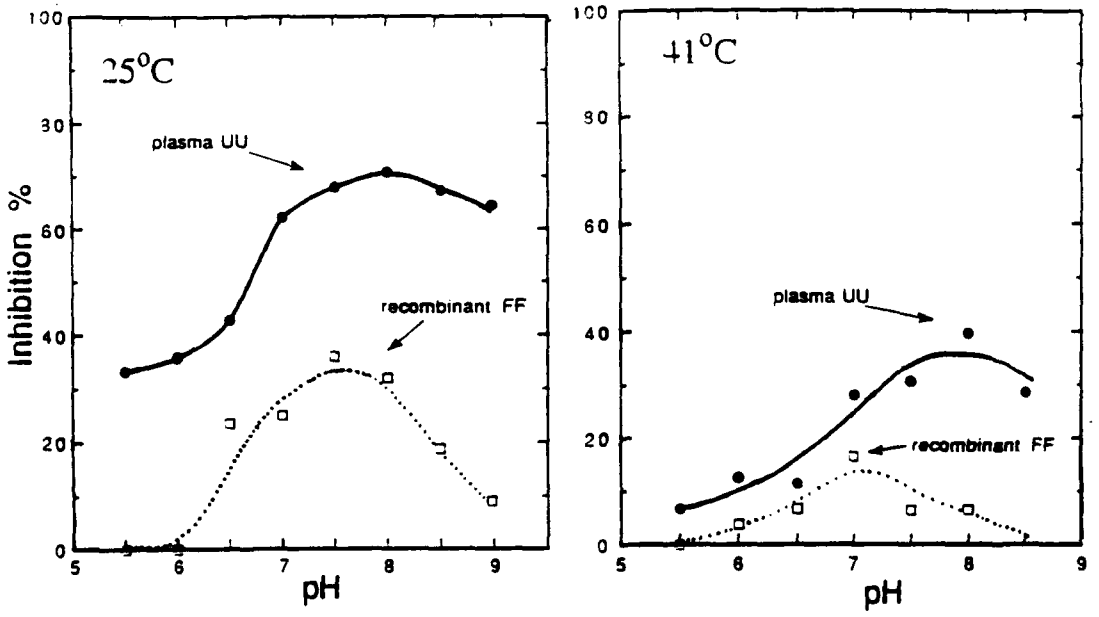

FIG. 4. **pH profile of inhibition by sodium fluoride.** Activity was measured with 50 μM benzoylcholine in the presence of 50 μM NaF at 25 and 41 °C. Points were obtained from the data in Fig. 2. Purified usual plasma BuChE, UU (●); recombinant fluoride-2 BuChE, FF (□).

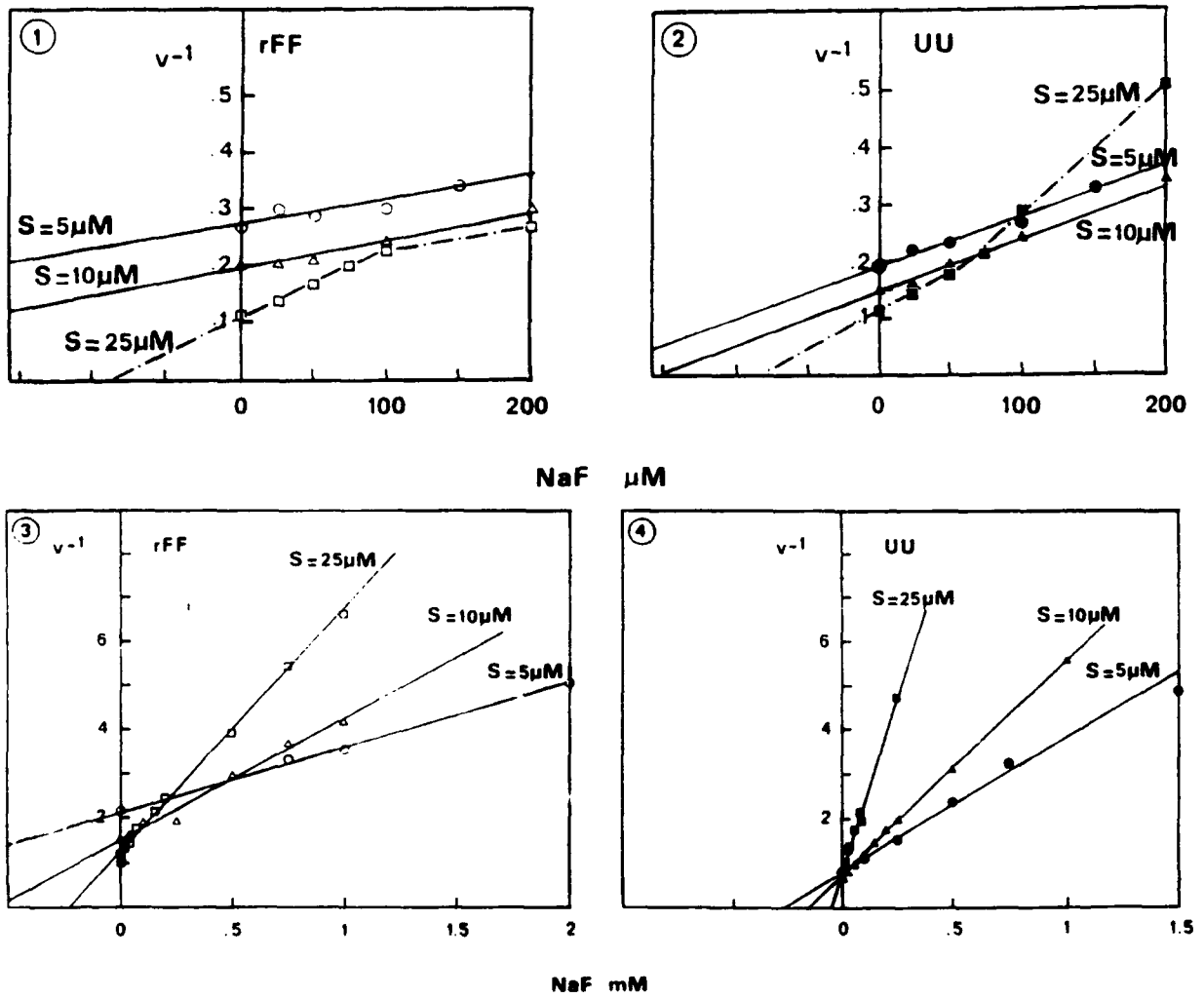

FIG. 5. **Dixon plots for inhibition by NaF of BuChE-catalyzed hydrolysis of benzoylcholine.** Benzoylcholine concentrations were 5 μM (○, ●), 10 μM (△, ▲), 25 μM (□, ■). In *panels 1* and 2 the buffer was 0.067 M potassium phosphate, pH 7.0, at 25 °C. In *panels 3* and *4* the buffer was 0.067 M potassium phosphate, pH 8.0, at 25 °C. Recombinant fluoride-2 BuChE, rFF, was used in *panels 1* and *3*. Purified plasma usual BuChE, UU, was used in *panels 2* and *4*. At low benzoylcholine concentration, uncompetitive K_i = 0.3 mM for rFF and uncompetitive K_i = 0.09 mM for UU.

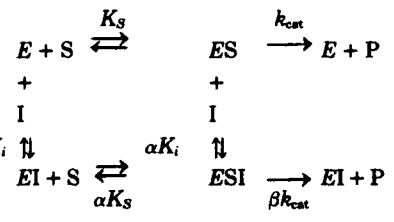

SCHEME II

K_s and K_i are the dissociation constants of enzyme-substrate and enzyme-inhibitor complexes, respectively. According to this scheme, in the absence of inhibitor, K_m and V_{max} represent apparent values of K_s and $k_{cat}E_o$. In the presence of inhibitor, *E*S and *E*SI are productive. The general velocity equation derived from rapid equilibrium assumptions (Ref. 17, p. 179) is:

$$v = \frac{V_{max}}{\frac{\left(1 + \frac{[I]}{\alpha K_i}\right)}{\left(1 + \frac{\beta[I]}{\alpha K_i}\right)} + \frac{K_s}{[S]}\frac{\left(1 + \frac{[I]}{K_i}\right)}{\left(1 + \frac{\beta[I]}{\alpha K_i}\right)}} \qquad \text{(Eq. 6)}$$

When $\alpha > 1$ and $0 < \beta < 1$ the reciprocal form of this equation gives a nonlinear plot as shown in Fig. 7. Inhibition constants and coefficients α and β were determined for dibucaine from secondary replots of 1/Δslope and 1/Δintercept *versus* 1/[I], where Δslope and Δintercept are the change in slope and in *y* intercept of the reciprocal of Equation 6, *i.e.* $1/v$ *versus* 1/[S] plots at different fixed inhibitor concentrations. This analysis showed nonlinear mixed inhibition of BuChE by dibucaine. The values of K_i were calculated to be 0.6 μM (α = 5.0, β = 0.5) for the purified plasma usual enzyme, 0.45 μM (α = 4.0, β = 0.44) for the recombinant usual enzyme, and 12.5 μM (α = 1.6, β = 0.7) for the recombinant fluoride variant. Since $\alpha_{uu} > \alpha_{FF}$, the competitive inhibition component is higher for the usual enzyme than for the fluoride-2 variant; inhibition of fluoride-2 BuChE is nearly nonlinear noncompetitive. The fact that the β inhibition coefficients for the two enzymes are of the same order of magnitude indicates that the ternary complexes *E*SI of both enzymes release product with a similar efficiency. This suggests that mutation G390V does not affect the covalent steps of enzyme catalysis. On the other hand, the actual affinity of the fluoride variant for dibucaine, which is 21-fold lower than that of the usual enzyme, confirms that the point mutation G390V strongly altered the binding of charged ligands to the enzyme active site gorge.

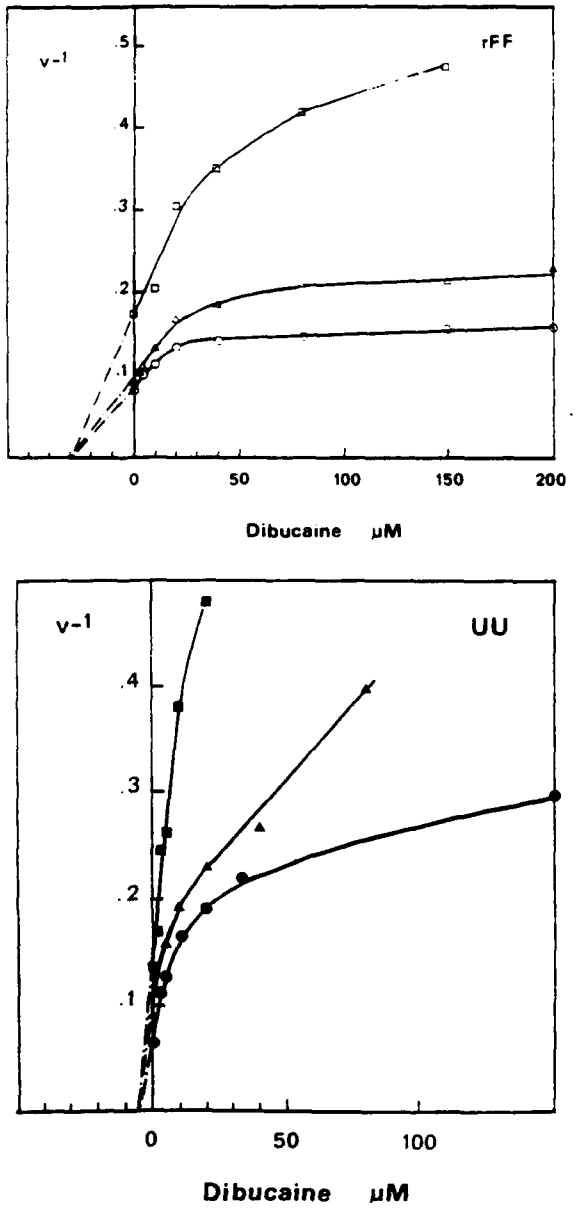

FIG. 6. **Dixon plots for inhibition by dibucaine of BuChE-catalyzed hydrolysis of *o*-nitrophenylacetate.** *Top*, recombinant fluoride-2 BuChE, rFF; *bottom*, purified usual plasma BuChE, UU. Concentrations of *o*-nitrophenylacetate were 0.2 mM (□, ■), 0.4 mM (△, ▲), and 0.6 mM (○, ●) in 0.067 M phosphate, pH 7.5, at 25 °C. All reactions contained 5.3% methanol. Apparent K_i = 30 μM for rFF, and 5 μM for UU.

An interesting feature is that for both enzymes, the replots of slope and intercept of Lineweaver-Burk plots *versus* [I] are not hyperbolic (Fig. 7). As expected for nonlinear inhibition, replots are curved but they do not reach a plateau with increasing dibucaine concentration. Indeed, for both enzymes, beyond a given dibucaine concentration (~25 μM for UU and ~75 μM for rFF) there is a decrease in $1/V_{maxi}$ indicating an "activating" effect of the inhibitor at high concentration, and there is a wavelike inflexion in the slope indicating an alteration in the inhibition mechanism. This unexpected behavior could be interpreted in terms of binding of a second inhibitor molecule to a regulatory site. Such a regulatory site has not been firmly demonstrated for BuChE. However, several lines of evidence argue for the existence of "peripheral" binding site(s) on the BuChE surface whose occupation alters the enzyme catalytic activity (42, 51–54).

Inhibition of butyrylthiocholine hydrolysis by amodiaquin was linear for both variants (Table IV). Thus, with the neutral ester, *o*-nitrophenylacetate, inhibition was nonlinear, but with the positively charged ester, butyrylthiocholine, inhibition by amodiaquin was linear. Substrate-dependent inhibition kinetic behavior has been observed for horse serum BuChE (41, 49, 50) and for AChE (55). The present data, showing that cationic ligands produced a partial nonlinear inhibition of BuChE-catalyzed hydrolysis of the neutral ester *o*-nitrophenylacetate, are consistent with the mechanistic models proposed for hydrolysis of positively charged substrates. They suggest that these ligands affect the enzyme reaction scheme by binding to vacant "anionic" site(s). Finally, whatever the intimate molecular mechanism of this inhibition, it is noteworthy that usual and fluoride-2 BuChE exhibited similar behavior and differed only in affinity for the inhibitors, with fluoride-2 BuChE consistently having weaker binding.

Kinetics of Progressive Inhibition—Progressive inhibition of usual plasma BuChE by iso-OMPA at pH 7.0 followed Scheme I and Equations 2 and 3 (Fig. 8). The calculated inhibition constants for usual BuChE were: $K_i = 60 \pm 16$ μM and $k_2 = 0.53 \pm 0.06$ min^{-1}. These values are in accordance with previously reported data (56). On the other hand, loss of activity of recombinant fluoride-2 BuChE (Fig. 9) did not follow reaction Scheme I. Instead, inhibition could be described by a two-exponential decay model:

$$\frac{e_t}{e_o} = \mathrm{A}e^{k_{i\mathrm{I}}t} + (1 - \mathrm{A})e^{k_{i\mathrm{II}}t} \qquad \text{(Eq. 7)}$$

A plot of k_{il} against iso-OMPA concentration (Fig. 8, *inset, dotted line*) gave a curve which was virtually superimposable on the curve for usual plasma BuChE (Fig. 8, *inset, solid line*). The inhibition constants for fluoride-2 BuChE were estimated to be $K_i = 72 \pm 35$ μM and $k_2 = 0.51 \pm 0.13$ min^{-1}. Thus, the inhibition constants by iso-OMPA for usual and fluoride-2 BuChE are very similar.

As regards the curved portion of Fig. 9, k_{iII} appeared to be roughly constant whatever the iso-OMPA concentration. When plots of log e_t/e_o *versus* t, such as the plot in Fig. 9, are curvilinear rather than linear, the curve can be interpreted as a reflection of inhibition of a multiple enzyme system (57). However, recombinant fluoride-2 BuChE is mostly a tetramer, arguing against multiple forms of BuChE being the source of catalytic heterogeneity. Thus, the curved plot suggests the presence in the CHO culture medium of competing enzymes which consume iso-OMPA. These enzymes could be organophosphate hydrolases and/or other targets of iso-OMPA such as serine enzymes. Evidence supporting the presence of several serine enzymes in the CHO cell culture medium was the observation of several [^{3}H]diisopropylfluorophosphate-labeled proteins on sodium dodecyl sulfate gels (data not shown). Additional support for the presence of competing enzymes came from the observation in Fig. 9 (*dashed line*) that preincubation of the CHO cell culture medium for 1 h with 5 mM EDTA significantly increased the inhibitory power of iso-OMPA. The EDTA might have neutralized an organophosphate hydrolase or a metal protease. Another possible explanation for the curvilinear plot, *i.e.* that the rate of reactivation (k_3 in Scheme I) was increased in the fluoride-2 variant, has not been ruled out.

Despite this uncertainty over the later portions of the time course in Fig. 9, the results from early time points show that reactivity of recombinant fluoride-2 BuChE with iso-OMPA was similar to reactivity of the usual plasma enzyme. Progressive inhibition by eserine confirmed this conclusion (data not shown). Finally, these results suggested that the reactivity

TABLE IV

Apparent inhibition constants for positively charged inhibitors of purified usual plasma BuChE (UU) and recombinant fluoride-2 BuChE (rFF)

Inhibitor	Substrate	pH[a]	K_i,app		K_i ratio	Type of inhibition
			UU	rFF		
			μM			
Tacrine	*o*-NPA[b]	7.5	0.0004[c]	0.0014	3.5	Nonlinear; competitive at low [I]
Dibucaine	*o*-NPA	7.5	5[d]	30	6	Nonlinear; noncompetitive at low [I]
Succinyldicholine	*o*-NPA	7.5	20[e]	125	6.25	Nonlinear; competitive at low [I]
Amodiaquin	*o*-NPA	7.5	25	80	3.2	Nonlinear; competitive at low [I]
Amodiaquin	BuSCh[f]	7.0	6	16	2.66	Linear; competitive

[a] 0.067 M phosphate, 25 °C.
[b] *o*-NPA, *ortho*-nitrophenylacetate.
[c] Literature values for tacrine inhibition: complex inhibition of acetylcholine hydrolysis at pH 8.0 and 25 °C with competitive (K_i = 0.0015 μM) at high substrate concentration and noncompetitive (K_i = 0.0056 μM) at low substrate concentration (47).
[d] Literature value for dibucaine inhibition: K_i = 2.7 μM in 0.067 M phosphate, pH 7.4, with 50 μM benzoylcholine (48).
[e] Literature value for succinyldicholine inhibition: K_i = 97.7 μM in 0.067 M phosphate, pH 7.4, with 50 μM benzoylcholine (49).
[f] BuSCh, butyrylthiocholine.

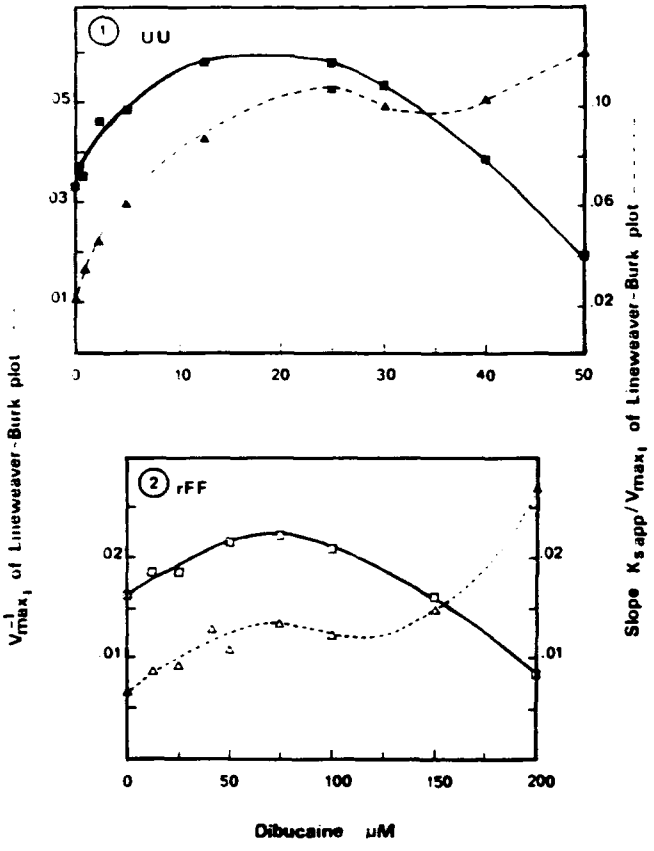

FIG. 7. **Secondary plots of data from Lineweaver-Burk plots for BuChE-catalyzed hydrolysis of *o*-nitrophenylacetate in the presence of various, fixed concentrations of dibucaine.** Lineweaver-Burk plots yielded intercepts for $1/V$max, and slopes for $K_{s_{app}}/V$max, which were plotted against dibucaine concentration. This plot shows that dibucaine gives nonlinear inhibition of *o*-nitrophenylacetate hydrolysis. Dibucaine concentrations above 25 μM for UU and 75 μM for rFF have an activating effect. $1/V$max$_i$, *continuous curves*; slope, *dashed curves*. *Panel 1*, purified usual BuChE; *panel 2*, recombinant fluoride-2 BuChE.

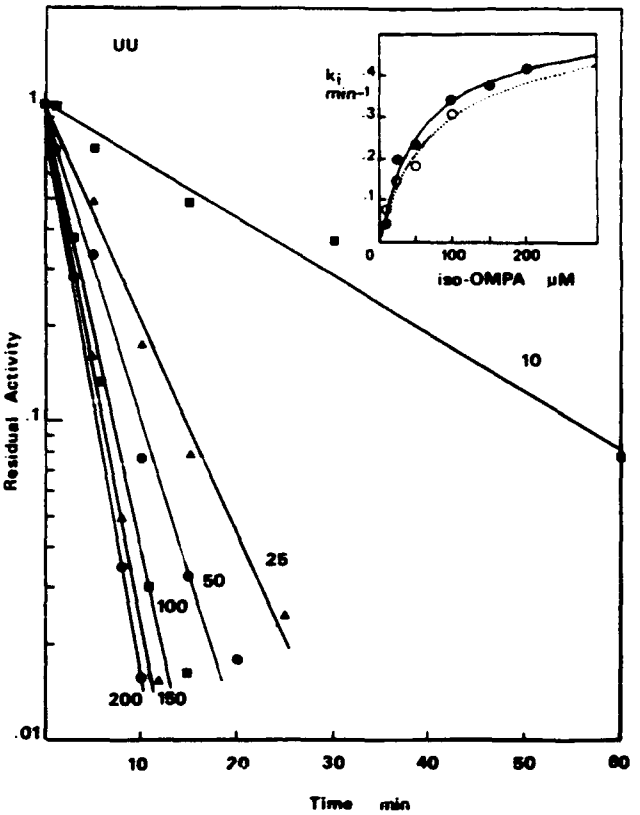

FIG. 8. **Progressive inhibition of purified usual plasma BuChE by iso-OMPA.** The semi-log plot shows residual activity toward butyrylthiocholine after incubation of BuChE with 10–200 μM iso-OMPA in 0.1 M phosphate, pH 7.0, at 25 °C, for various lengths of time. Each reaction contained 0.01 μM active sites of purified usual plasma BuChE, UU. *Numbers* on *lines* are iso-OMPA concentrations (μM). The lines were drawn by fitting the data to Equation 2, thus yielding an apparent k_i value for each iso-OMPA concentration. *Inset of Fig. 8*: saturation plot of apparent phosphorylation rate constant against iso-OMPA concentration. The *solid circles* (●) are apparent k_i values for usual BuChE; the *solid line* represents a fit of apparent k_i values to Equation 3 for usual plasma BuChE. The *open circles* (○) are the apparent k_{i1} values for fluoride-2 BuChE taken from the initial slopes of the lines in Fig. 9. The *dotted line* is a fit of these apparent k_{i1}values to Equation 3. For usual BuChE, K_i = 60 ± 16 μM, k_2 = 0.53 ± 0.06 min^{-1}.

of the active site serine was not altered by the mutation Gly[390] to Val. If this statement could be generalized to other fluoride-2 BuChE-catalyzed reactions, then the kinetic behavior differences observed between usual and fluoride-2 BuChE could be explained in terms of K_m and K_i. In other words, it may be hypothesized that the mutation alters only the binding prop-

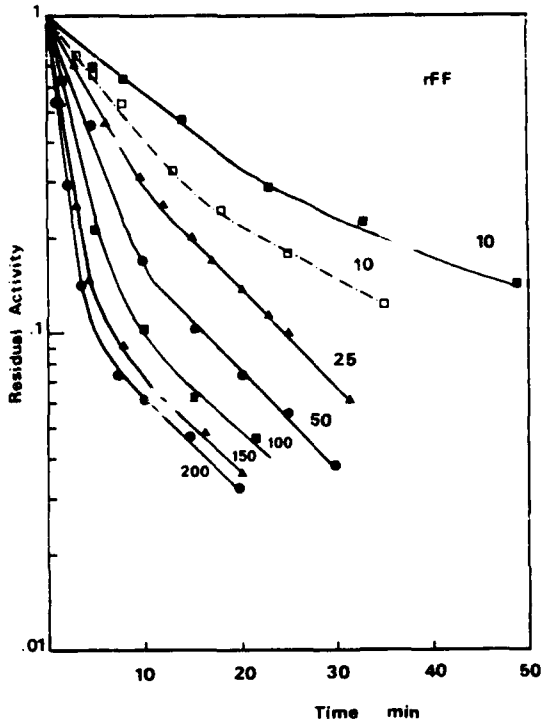

FIG. 9. **Progressive inhibition of recombinant fluoride-2 BuChE by iso-OMPA.** The semi-log plot shows residual activity toward butyrylthiocholine after incubation of BuChE with 10–200 μM iso-OMPA in 0.1 M phosphate, pH 7.0, at 25 °C for various lengths of time. Each reaction contained 0.003 μM active sites of recombinant fluoride-2 BuChE, rFF. The curves were drawn by fitting the data to Equation 7. Apparent k_{i1} values calculated from the initial slopes were used in the *inset* of Fig. 8. *Dashed curve*: inhibition started after 1 h of preincubation with 5 mM EDTA. *Numbers* on *curves* are iso-OMPA concentrations (μM). For fluoride-2 BuChE, $K_i = 72 \pm 35$ μM, $k_2 = 0.51 \pm 0.13$ min^{-1}.

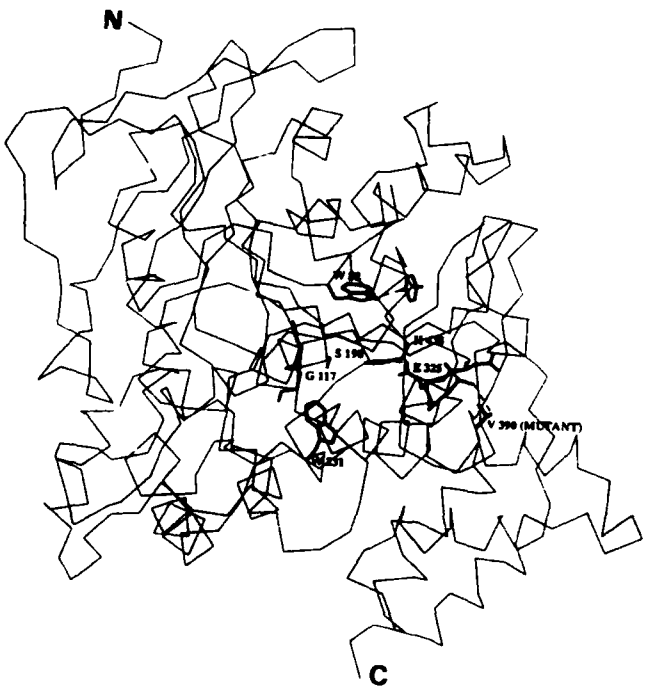

FIG. 10. **Three-dimensional carbon α trace of modeled human BuChE monomer.** The catalytic triad amino acids (S198, H438, E325) are highlighted as well as G117 whose main chain nitrogen is a part of the oxyanion hole. Two amino acids important for binding of the positively charged moiety of substrates and ligands are W82 and W231. W82 is hydrogen-bonded to Y440. The mutation in the fluoride-2 variant, G390V, is located on the αF helix. Amino acids are numbered from the N-terminal of mature human BuChE (43). Corresponding amino acid numbers for *Torpedo* AChE are S200, H440, E327, G119, W84, W233, Y442, and D392.

erties of the enzyme active pocket. The small, apparent shifts in the enzyme pK_a shown in Fig. 2, which we have attributed to histidine 438 of the catalytic triad, do not appear to be large enough to affect the rates of reaction between BuChE and either iso-OMPA or eserine at pH 7.0.

Molecular Modeling—Modeling of human BuChE by Harel *et al.* (58) gave a structure superimposable on the 3-D crystallographic structure of *Torpedo* AChE. The Gly^{390} Val mutation is located in the middle of the αF helix (Fig. 10). In an attempt to explain the reduced affinity of the fluoride-2 variant, we have used the BuChE model to simulate the interaction of BuChE with succinyldicholine (Fig. 11) and of BuChE with dibucaine in the presence of *o*-nitrophenylacetate (Fig. 12).

The G390V mutation induces no steric hindrances in the model of the fluoride-2 variant, and there is no indication that it could affect either folding or stability of the variant. Nevertheless, as Gly^{390} faces the catalytic triad of BuChE, we propose the following hypotheses to link the biochemical and structural properties of this mutant.

The G390V mutation could affect the position of Glu^{325} of the catalytic triad, if one assumes that BuChE and *Torpedo* AChE do not have the same packing. Solvent isotope effect on kinetics and proton inventory suggest that this glutamate, rather than participating in a charge relay system, may stabilize histidine during catalysis (59). As shown in Fig 11*a*, the G390V mutation could perturb hydrogen bonds between the oxygen O on the peptide bond carbonyl of Asp^{324} and the hydroxyl group OG2 of Thr^{327}, and also between the same Asp^{324} oxygen atom and NH in the peptide bond of His*438*. Since these hydrogen bonds stabilize the acid turn (60) on which Glu^{325} is located, a weakening of these bonds may alter the position and/or reactivity of His^{438}. Thus, the G390V mutation could change the relationship between Glu^{325} and His*438*. This view could explain the observed slight shift in pK_a of His^{438}.

As described in Fig. 11 amino acids Trp^{82}, His^{438}, Gly^{439}, and Tyr^{440} are involved in the binding of one of the choline heads of succinyldicholine. A displacement of His^{438} could move Tyr^{440} away from Trp^{82}, with the result of a weaker affinity for substrates and ligands. However, this hypothesis is doubtful. It supposes significant movement of His^{438}, which would imply important changes in the catalytic properties of the mutant. These changes were not observed. The second choline head of succinyldicholine interacts with Trp^{231}. Molecular modeling provides no evidence that the orientation of Trp^{231} is changed in the mutant enzyme.

A second hypothesis to explain the low affinity of this mutant suggests that the G390V mutation weakens the interaction between Asp^{70} and Tyr^{332} and alters the transducer function of these amino acids. The G390V mutation could change the hydrogen bond network around Thr^{327} and thus change the beginning of the αF′1 helix on which are located Ala^{328}, Phe^{329}, and Tyr^{332}. In *Torpedo* and electric eel AChE, the amino acids in equivalent positions (Phe^{330}, Phe^{331}, and Tyr^{334}) are assumed to play an important role in the binding of substrate and ligand (19, 61).

Ala^{328}, Phe^{329}, and Tyr*332* appear to be more than 5 Å from the Trp^{82} aromatic cluster and the substrate choline head. It could nevertheless be supposed that displacement of the αF′1 helix could affect Tyr^{332} which is hydrogen-bonded to Asp^{70} in the gorge surface 10 Å distant from the Trp*82* aromatic

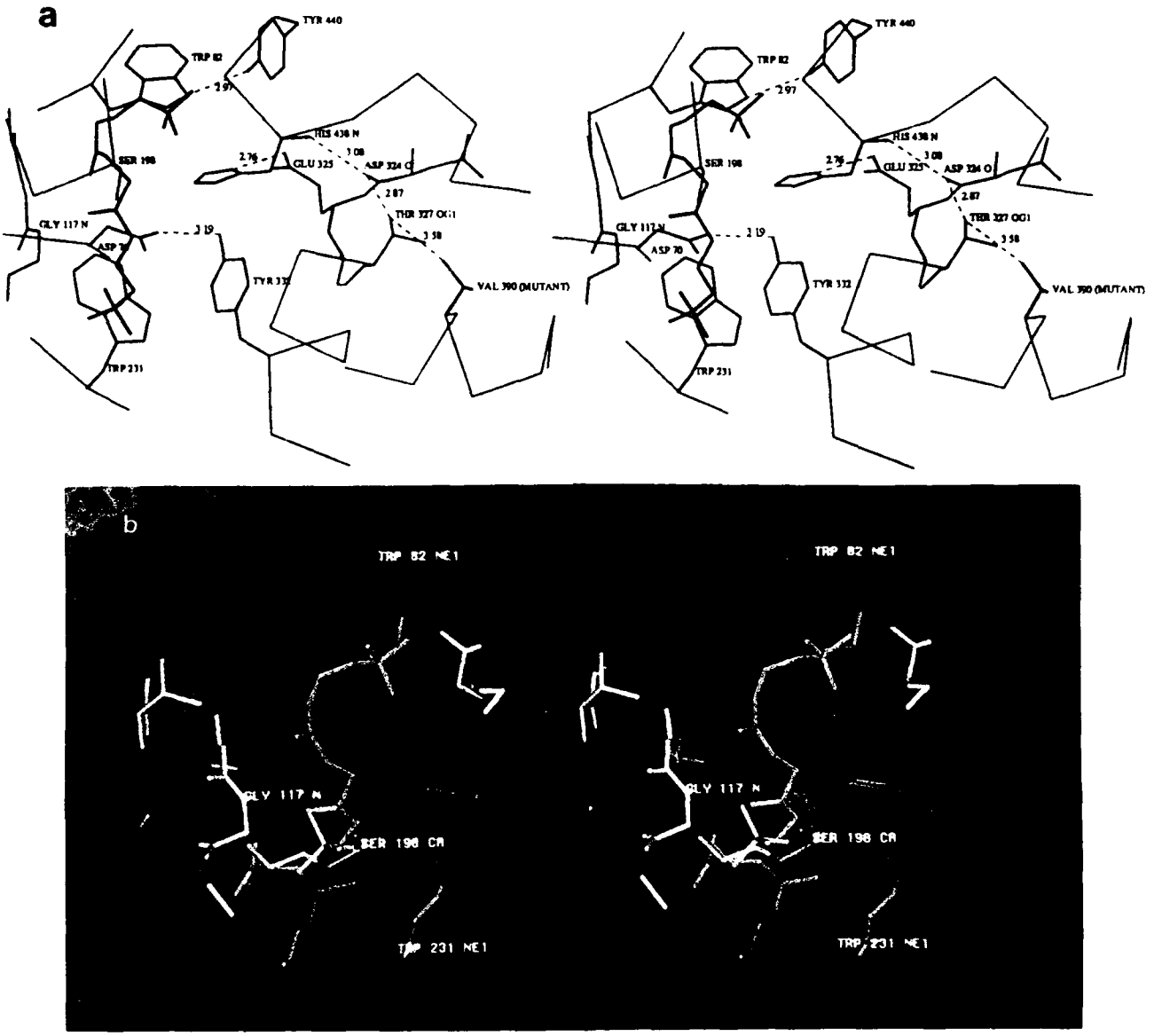

FIG. 11. **Stereo view of succinyldicholine in the active site gorge of modeled human BuChE.** *a*, close-up view of the G390V mutation and its relation to the active site. One choline head of succinyldicholine interacts with Trp^{82}, with the peptide bond carbonyl of Gly^{439}, and with the peptide bond carbonyl of His^{438}. Trp^{82} is hydrogen-bonded to Tyr^{440}. The presence of Leu^{286} and Val^{288} in human BuChE in place of Phe^{288} and Phe^{290} in *Torpedo* AChE reduces steric constraints in the BuChE active site gorge and allows a weak (4 Å) cation-aromatic interaction between the second choline head and Trp^{231}. The two carbonyls of succinic acid are hydrogen-bonded to NH in the peptide bonds of Gly^{116} and Gly^{117}. These carbonyls form a solid angle of 60°. The carbonyl susceptible to nucleophilic attack by Ser^{198} has been placed in a tetragonal conformation at 1.6 Å from OG2 of Ser^{198}. Numbers under dashed lines are distances expressed in Ångstroms. *b*, photograph. Amino acids are colored according to their type: acidic, *red*; basic, *blue*; aromatic, *magenta*; aliphatic, *yellow*; and *green* for other residues. Succinyldicholine is *dark yellow*. The Connolly's surface of the enzyme is represented by *red* points to a 1.6 Å probe sphere, while the Van der Waals surface of succinyldicholine is *green*.

binding site. It should be remembered that mutation of Asp*70* to Gly in human BuChE determines the "atypical" variant (62). People carrying the Asp^{70} Gly mutation experience hypersensitivity to succinyldicholine because of reduced affinity for this drug (4, 6). As suggested from site-directed mutagenesis of human AChE (63), these two amino acids (Tyr^{341} and Asp^{74} in human AChE) could be involved in signal transduction of substrate-induced conformational changes following initial binding to the cholinesterase active surface. Thus, displacement of the beginning of helix $\alpha F'1$ could affect the conformational plasticity of amino acids involved in the binding process (Fig. 11). Dislocation of the interaction between Asp^{70} and Tyr^{332} and weakening of the signal transduction mechanism could explain the reduced affinity of the fluoride-2 variant for charged substrates and ligands. As modeling does not allow a clear understanding of the properties of the fluoride-2 variant, crystallization of human BuChE is underway.

DISCUSSION

The purpose of this work was to investigate the effect of the point mutation Gly^{390} to Val on the kinetic properties of BuChE. This point mutation is naturally present in the fluoride-2 variant of human BuChE, and its presence is associated with an abnormal response to succinyldicholine (reviewed in Ref. 6).

The fluoride number and dibucaine number (percent inhibition of benzoylcholine hydrolysis by 50 μM NaF or 50 μM dibucaine) of the recombinant fluoride-2 BuChE were 36 and 66, respectively. These values are in agreement with fluoride

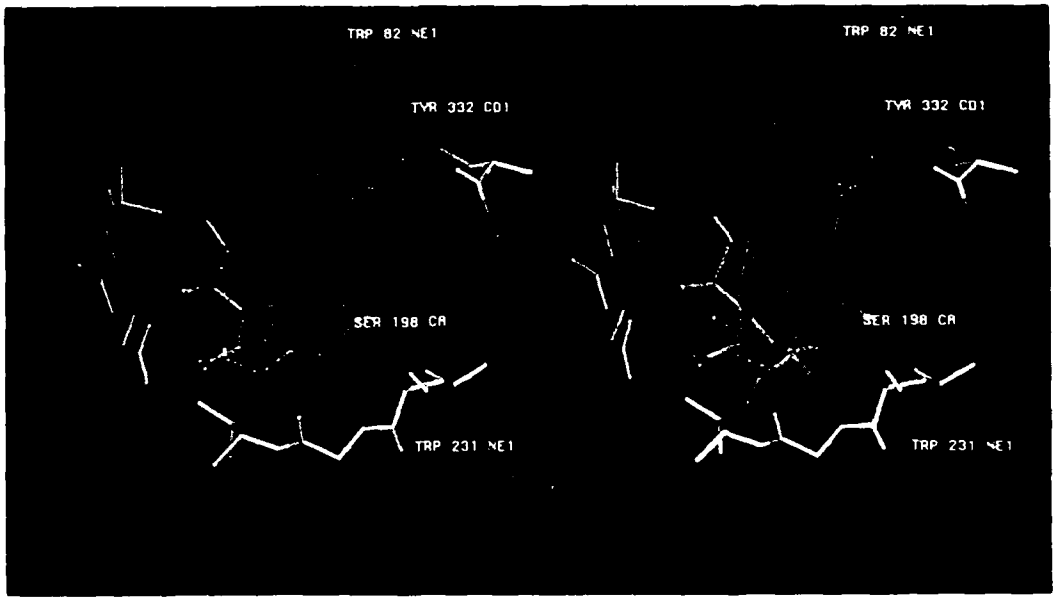

FIG. 12. **Photograph showing *o*-nitrophenylacetate and dibucaine in the active site gorge.** Substrate and ligand are *dark yellow*. The Connolly's surface of butyrylcholinesterase is represented by *dark blue* points to a 1.6-Å probe sphere. The Van der Waals surface of dibucaine is *red* and that of *o*-nitrophenylacetate is *green*. Modeling clearly shows that the BuChE active site gorge can accommodate *o*-nitrophenylacetate and dibucaine simultaneously. *o*-Nitrophenylacetate is modeled at 1.6 Å from Ser^{198}; its nitro group is hydrogen-bonded to protonated $Glu^{?}$. The initial extended conformation of *o*-nitrophenylacetate was not changed during the refinement process. The aromatic ring of dibucaine interacts with $Trp^{?}$, its protonated tertiary amine group with $Trp^{?}$, and its carbonyl with Gly^{117} and Gly^{116} amides. In the presence of *o*-nitrophenylacetate these interactions are not optimal. The dibucaine molecule rotates about 20° and the only significant interaction is with $Trp^{?}$.

numbers of 34–35 and dibucaine numbers of 64–68 for the three published homozygous fluoride plasma samples (64–66). This indicates that the kinetic behavior of the recombinant enzyme is not dependent on posttranslational modifications, such as glycosylation, that occurred in CHO cells. No other comparisons are possible because no other kinetic data for the fluoride variants of plasma BuChE have been published.

The secreted recombinant fluoride-2 BuChE acquired proteolytic nicks during storage of serum-free culture medium. These proteolytic nicks did not appear to affect kinetic parameters. A similar conclusion regarding the unimportance of proteolytic nicks was made by Cauet *et al.* (67) who determined that the trypsin-generated monomer of horse serum BuChE behaved with identical kinetic parameter values as the native tetrameric enzyme. Our results are for the tetrameric form of recombinant fluoride-2 BuChE, since despite proteolysis most of the recombinant BuChE was a tetramer.

The kinetic data we report show that the $Gly^{?}$ to Val mutation did not dramatically change the behavior of the enzyme. Although the pK_i of the fluoride-2 BuChE was slightly lower than the pK_i of the usual plasma BuChE, the reactivity of fluoride-2 BuChE with the irreversible organophosphate inhibitor iso-OMPA was similar to that of usual BuChE, suggesting that catalytic activity of usual and fluoride-2 BuChE did not differ markedly. In fact, the only significant differences between usual and fluoride-2 BuChE concerned their K_m, K_i, and α coefficient of mixed-type inhibition for dibucaine inhibition of *o*-nitrophenylbutyrate hydrolysis. Ratios of these apparent parameters fluctuated between 1.5 and 6 depending on the substrate and inhibitor nature. This indicated that the fluoride-2 BuChE bound neutral and charged substrates and ligands less tightly than the usual BuChE.

Molecular modeling to understand the molecular basis of the remote effect of the $Gly^{?}$ to Val mutation upon the binding affinity of BuChE suggested two hypotheses. One hypothesis is that the mutation exerts an indirect effect on the position of $Glu^{?}$, which in turn slightly alters the pK_i of $His^{?}$. The altered position of $Glu^{?}$ could induce displacement of $Tyr^{?}$ which is hydrogen bonded to $Trp^{?}$. A second, more likely, hypothesis is that the mutation alters the beginning of helix αF1, which in turn could dislocate the hydrogen bond between $Asp^{?}$ and $Tyr^{?}$. This may weaken the binding of charged substrates and reduce signal transduction capability. These tentative explanations from molecular modeling need to be verified by x-ray analysis of the BuChE crystal structure.

As regards the question of hypersensitivity to succinyldicholine, one can calculate that after intravenous injection of a clinical dose of succinyldicholine (1 mg/kg), the initial plasma concentration of succinyldicholine is close to 20 mg/liter, that is 50 μM (68). Since the apparent K_i of fluoride-2 BuChE for this compound is 125 μM (Table IV), the rate of hydrolysis of succinyldicholine by this variant should be slow when the concentration of the muscle relaxant is in the pharmacologic range. Thus, the low affinity of fluoride-2 BuChE for succinyldicholine could explain the moderate succinyldicholine hypersensitivity of people carrying this variant.

Acknowledgments—We thank Dr. J. Sussman and Dr. M. Harel (Weizmann Institute of Science, Rehovot, Israel) for the coordinates of the three-dimensional structure of *T. californica* AChE and for the coordinates of their human BuChE model. Expression plasmid pD5 was a gift from Dr. K. Berkner, ZymoGenetics, Seattle, WA.

REFERENCES

1. Arpagaus, M., Kott, M., Vatsis, K. P., Bartels, C. F., La Du, B. N., and Lockridge, O. (1990) *Biochemistry* **29**, 124–131
2. Allderdice, P. W., Gardner, H. A. R., Galutira, D., Lockridge, O., La Du, B. N., and McAlpine, P. J. (1991) *Genomics* **11**, 452–454
3. Gaughan, G., Park, H., Priddle, J., Craig, I., and Craig, S. (1991) *Genomics* **11**, 455–458
4. Lockridge, O. (1990) *Pharmacol. & Ther.* **47**, 35–60
5. La Du, B. N., Bartels, C. F., Nogueira, C. P., Arpagaus, M., and Lockridge,

O. (1991) *Cell. Mol. Neurobiol.* **11**, 79–89
6. Whittaker, M. (1986) *Cholinesterase*, Karger, Basel
7. Harris, H., and Whittaker, M. (1961) *Nature* **191**, 496–498
8. Nogueira, C. P., Bartels, C. F., McGuire, M. C., Adkins, S., Lubrano, T., Rubinstein, H. M., Lightstone, H., Van Der Spek, A. F. L., Lockridge, O., and La Du, B. N. (1992) *Am. J. Hum. Genet.* **51**, 821–828
9. Kalow, W., and Lindsay, H. A. (1955) *Can. J. Biochem. Physiol.* **33**, 568–574
10. Powell, J. S., Berkner, K. L., Lebo, R. V., and Adamson, J. W. (1986) *Proc. Natl. Acad. Sci. U. S. A.* **83**, 6465–6469
11. McTiernan, C., Adkins, S., Chatonnet, A., Vaughan, T. A., Bartels, C. F., Kott, M., Rosenberry, T. L., La Du, B. N., and Lockridge, O. (1987) *Proc. Natl. Acad. Sci. U. S. A.* **84**, 6682–6686
12. Urlaub, G., Mitchell, P. J., Kas, E., Chasin, L. A., Funanage, V. L., Myoda, T. T., and Hamlin, J. (1986) *Somatic Cell Mol. Genet.* **12**, 555–566
13. Kozak, M. (1991) *J. Biol. Chem.* **266**, 19867–19870
14. Dietz, A. A., Rubinstein, H. M., Lubrano, T., and Hodges, L. K. (1972) *Am. J. Hum. Genet.* **24**, 58–64
15. Ellman, G. L., Courtney, K. D., Andres, V., Jr., and Featherstone, R. M. (1961) *Biochem. Pharmacol.* **7**, 88–95
16. Zapf, P. W., and Coghlan, Ch. M. (1973) *Clin. Chim. Acta* **44**, 237–242
17. Segel, I. H. (1975) *Enzyme Kinetics*, pp. 100–286, John Wiley & Sons, Inc., New York
18. Kitz, R., and Wilson, I. B. (1962) *J. Biol. Chem.* **237**, 3245–3249
19. Sussman, J. L., Harel, M., Frolow, F., Oefner, C., Goldman, A., Toker, L., and Silman, I. (1991) *Science* **253**, 872–879
20. Roussel, A., and Cambillau, C. (1989) in *Silicon Graphics Geometry Partner Directory* (Silicon Graphics, ed) pp. 77–78, Silicon Graphics, Mountain View, CA
21. Brunger, A. T., Kuriyan, J., and Karplus, M. (1987) *Science* **235**, 458–460
22. Jensen, B. (1976) *Acta Chem. Scand.* **B30**, 1002–1004
23. Hayward, B. S., and Donohue, J. (1977) *J. Cryst. Mol. Struct.* **7**, 275–294
24. Allen, F. H., Kennard, O., and Taylor, R. (1983) *Acc. Chem. Res.* **16**, 146–153
25. Allen, F. H., Bellard, S., Brice, M. D., Cartwright, B. A., Doubleday, A., Higgs, H., Hummelink-Peters, T., Kennard, O., Motherwell, W. D. S., Rodgers, J. R., and Watson, D. G. (1979) *Acta Crystallogr. Sect. B Struct. Sci.* **B35**, 2331–2339
26. Guttormson, R., and Robertson, B. E. (1979) *Acta Crystallogr. Sect. B Struct. Sci.* **B28**, 2702–2708
27. Connolly, M. L. (1983) *Science* **221**, 709–713
28. Lockridge, O., and La Du, B. N. (1978) *J. Biol. Chem.* **253**, 361–366
29. Ferro, A., and Masson, P. (1987) *Biochim. Biophys. Acta* **916**, 193–199
30. McComb, R. B., La Motta, R. V., and Wetstone, H. J. (1965) *Clin. Chem.* **11**, 645–652
31. Main, A. R. (1961) *Biochem. J.* **79**, 246–252
32. Bamford, K. F., and Harris, H. (1964) *Ann. Hum. Genet.* **27**, 417–425
33. Valentino, R. J., Lockridge, O., Eckerson, H. W., and La Du, B. N. (1981) *Biochem. Pharmacol.* **30**, 1643–1649
34. Kalow, W. (1964) *Can. J. Physiol. Pharmacol.* **42**, 161–168
35. Page, J. D., Wilson, I. B., and Silman, I. (1985) *Mol. Pharmacol.* **27**, 437–443
36. Gatley, S. J. (1991) *Biochem. Pharmacol.* **41**, 1249–1254
37. Wetherell, J. R., and French, M. C. (1986) *Biochem. Parmacol.* **35**, 939–945
38. Özer, N., and Özer, J. (1987) *Arch. Biochem. Biophys.* **255**, 89–94
39. Hersh, L. B., Raj, P. P., and Ohlweiler, D. (1974) *J. Pharmacol. Exp. Ther.* **189**, 544–549
40. Christian, S. T., and Beasley, J. G. (1968) *J. Pharm. Sci.* **57**, 1025–1027
41. Eriksson, H., and Augustinsson, K.-B. (1979) *Biochim. Biophys. Acta* **567**, 161–173
42. Cauet, G., Friboulet, A., and Thomas, D. (1987) *Biochem. Cell Biol.* **65**, 529–535
43. Lockridge, O., Bartels, C. F., Vaughan, T. A., Wong, C. K., Norton, S. E., and Johnson, L. L. (1987) *J. Biol. Chem.* **262**, 549–557
44. Gibney, G., Camp, S., Dionne, M., MacPhee-Quigley, K., and Taylor, P. (1990) *Proc. Natl. Acad. Sci. U. S. A.* **87**, 7546–7550
45. Heilbronn, H. (1965) *Acta Chem. Scand.* **19**, 1333–1346
46. Brestkin, A. P., and Fruentova, T. A. (1968) *Biokhimiya* **33**, 817–822
47. Heilbronn, E. (1961) *Acta Chem. Scand.* **15**, 1386–1390
48. Kalow, W., and Davies, R. O. (1958) *Biochem. Pharmacol.* **1**, 183–192
49. Söylemez, Z., and Özer, I. (1984) *Arch. Biochem. Biophys.* **235**, 650–656
50. Söylemez, Z., and Özer, I. (1985) *Comp. Biochem. Physiol.* **81C**, 433–437
51. Narayanan, R., and Balaram, P. (1981) *Int. J. Pept. Protein Res.* **17**, 170–180
52. Gaal, J., Bartha, F., and Batke, J. (1983) *Eur. J. Biochem.* **135**, 157–162
53. Masson, P., and Balny, C. (1988) *Biochim. Biophys. Acta* **954**, 208–215
54. Cléry, C., Masson, P., Heiber-Langer, I., and Balny, C. (1992) *Biochim. Biophys. Acta* **1159**, 295–302
55. Berman, H. A., and Leonard, K. (1990) *Biochemistry* **29**, 10640–10649
56. Aldridge, W. N. (1953) *Biochem. J.* **53**, 62–67
57. Main, A. R. (1969) *J. Biol. Chem.* **244**, 829–840
58. Harel, M., Sussman, J. L., Krejci, E., Bon, S., Chanal, P., Massoulié, J., and Silman, I. (1992) *Proc. Natl. Acad. Sci. U. S. A.* **89**, 10827–10831
59. Pryor, A. N., Selwood, T., Leu, L.-S., Andracki, M. A., Lee, B. H., Rao, M., Rosenberry, T., Doctor, B. P., Silman, I., and Quinn, D. M. (199?) *J. Am. Chem. Soc.* **114**, 3896–3900
60. Ollis, D. L., Cheah E., Cygler, M., Dijkstra, B., Frolow, F., Franken, S. M., Harel, M., Remington, S. J., Silman, I., Schrag, J., Sussman, J. L., Verschueren, K. H. G., and Goldman, A. (1992) *Protein Eng.* **5**, 197–211
61. Sussman, J. L., and Silman, I. (1992) *Curr. Opin. Struct. Biol.* **2**, 721–729
62. McGuire, M. C., Nogueira, C. P., Bartels, C. F., Lightstone, H., Hajra, A., Van der Spek, A. F. L., Lockridge, O., and La Du, B. N. (1989) *Proc. Natl. Acad. Sci. U. S. A.* **86**, 953–957
63. Shafferman, A., Velan, B., Ordentlich, A., Kronman, C., Grosfeld, H., Leitner, M., Flashner, Y., Cohen, S., Barak, D., and Ariel, N. (1992) *EMBO J.* **11**, 3561–3568
64. Lehmann, H., Liddell, J., Blackwell, B., O'Connor, D. C., and Daws, A. V. (1963) *Br. Med. J.* **i**, 1116–1118
65. Liddell, J., Lehmann, H., and Davies, D. (1963) *Acta Genet. Basel* **13**, 95–108
66. Whittaker, M. (1964) *Acta Genet. Basel* **14**, 281–285
67. Cauet, G., Friboulet, A., and Thomas, D. (1987) *Biochim. Biophys. Acta* **912**, 338–342
68. Kalow, W. (1959) *Anesthesiology* **20**, 505–518